

Sources and export of particle-borne OM during a monsoon flood in a catchment of northern Laos

E. Gourdin et al.

Sources and export of particle-borne organic matter during a monsoon flood in a catchment of northern Laos

E. Gourdin¹, S. Huon², O. Evrard¹, O. Ribolzi³, T. Bariac⁴,
O. Sengtaheuanghoung⁵, and S. Ayrault¹

¹Laboratoire des Sciences du Climat et de l'Environnement (LSCE), UMR 8212 (CEA-CNRS-UVSQ-IPSL), Domaine du CNRS, avenue de la Terrasse, 91198 Gif-sur-Yvette cedex, France

²Université Pierre et Marie Curie (UPMC), UMR 7618 iEES (UPMC-CNRS-IRD-INRA-Université Paris 7-UPEC), case 120, 4 place Jussieu, 75252 Paris cedex 05, France

³IRD, Géosciences Environnement Toulouse (GET), UMR 5563 (CNRS-UPS-IRD), 14 avenue Edouard Belin, 31400 Toulouse, France

⁴CNRS, UMR 7618 iEES (UPMC-CNRS-IRD-INRA-Université Paris 7-UPEC), campus INRA – AgroParisTech, Bâtiment EGER, 78550 Thiverval – Grignon, France

⁵Department of Agriculture Land Management (DALam), P.O. Box 4199, Ban Nongviengkham, Xaythany District, Vientiane, Lao PDR

Title Page

Abstract

Introduction

Conclusions

References

Tables

Figures

◀

▶

◀

▶

Back

Close

Full Screen / Esc

Printer-friendly Version

Interactive Discussion

Received: 26 May 2014 – Accepted: 29 May 2014 – Published: 17 June 2014

Correspondence to: E. Gourdin (elian.gourdin@lsce.ipsl.fr)

Published by Copernicus Publications on behalf of the European Geosciences Union.

BGD

11, 9341–9378, 2014

**Sources and export
of particle-borne OM
during a monsoon
flood in a catchment
of northern Laos**

E. Gourdin et al.

Title Page

Abstract

Introduction

Conclusions

References

Tables

Figures



Back

Close

Full Screen / Esc

Printer-friendly Version

Interactive Discussion



Abstract

Tropical rivers of Southeast Asia are characterized by high specific carbon yields and supplies to the ocean. The origin and dynamics of particulate organic matter were studied in the Houay Xon River catchment located in northern Laos during the first erosive flood of the rainy season in May 2012. The partly cultivated catchment is equipped with three successive gauging stations draining areas ranging between 0.2 and 11.6 km² on the main stem of the permanent stream, and two additional stations draining 0.6 ha hillslopes. In addition, the sequential monitoring of rainwater, overland flow and suspended organic matter compositions was realized at 1 m² plot scale during a single storm. The composition of particulate organic matter (total organic carbon, total nitrogen, $\delta^{13}\text{C}$ and $\delta^{15}\text{N}$) was determined for suspended sediment, soil surface and subsurface samples collected in the catchment ($n = 57, 65$ and 11 respectively). Hydrograph separation of event water was conducted using water electric conductivity and $\delta^{18}\text{O}$ data measured for rainfall, overland flow and river water base flow ($n = 9, 30$ and 57 , respectively). The composition of particulate organic matter indicates that upstream suspended sediments were mainly derived from cultivated soils labelled by their C_3 vegetation cover (upland rice, fallow vegetation and teak plantations) but that collapsed riverbanks, characterized by C_4 vegetation occurrence (Napier grass), significantly contributed to sediment yields during water level rise and at the downstream station. The highest runoff coefficient (11.7%), sediment specific yield (433 kg ha⁻¹), total organic carbon specific yield (8.3 kg C ha⁻¹) and overland flow contribution (78–100%) were found for the reforested areas covered by teak plantations. Total organic carbon specific yields were up to 2.6-fold higher (at downstream station) than the annual ones calculated 10 years earlier, before the expansion of teak plantations in the catchment. They may be attributed both to the sampling period at the onset of the rainy season (following field clearing by slash and burn) and to the impact of land use change during the past decade.

Sources and export of particle-borne OM during a monsoon flood in a catchment of northern Laos

E. Gourdin et al.

Title Page

Abstract

Introduction

Conclusions

References

Tables

Figures



Back

Close

Full Screen / Esc

Printer-friendly Version

Interactive Discussion



1 Introduction

Soil is the largest terrestrial reservoir of carbon, exceeding biosphere and atmosphere storage capacities (e.g., Sarmiento and Gruber, 2002). Although tropical soils account for ca. 30% of the total carbon storage (e.g., Dixon et al., 1994; Zech et al., 1997), high intensity storms (e.g., Goldsmith et al., 2008; Thothong et al., 2011) as well as deforestation and land use change are responsible for high soil carbon losses and deliveries by rivers. For example Houghton (1991) estimated that deforestation in Laos, the sixth most affected tropical country according to the FAO/UNEP (1981), released ca. 85×10^{12} g C yr⁻¹ to the atmosphere from 1979 to 1989. Degens et al. (1991) identified the Asian tropical rivers as the main contributors of dissolved and particulate matter to world oceans, far before South American rivers. More recently, Huang et al. (2012) estimated that tropical rivers of Asia have the highest specific carbon yield in which ca. 25% of the delivery is made of particulate organic matter. This latter component does not vary linearly with total suspended sediment load (Ludwig et al., 1996), indicating that particulate organic matter is diluted by high concentrations of mineral matter that is supplied to the rivers through soil and/or riverbank erosion processes along river courses. Small mountainous headwater catchments play a key role in the delivery pattern because they are characterized by high specific discharges and sediment loads (Milliman and Syvitski, 1992). In this context, processes that control organic matter export from tropical catchments should be better understood and constrained, as they account for a significant component in the drawdown or emission of carbon dioxide (Lal, 2003).

Tropical storms may also result in the supply of large quantities of suspended sediment to streams (Descroix et al., 2008; Evrard et al., 2010) and lead to numerous problems downstream (Syvitski et al., 2005). Sediments can accumulate behind dams, which results in the siltation of water reservoirs (Downing et al., 2008; Thothong et al., 2011). Suspended organic matter also contributes to water quality degradation (Tanik et al., 1999) playing thereby a major role in nutrient biogeochemical cycles (Quinton

BGD

11, 9341–9378, 2014

Sources and export of particle-borne OM during a monsoon flood in a catchment of northern Laos

E. Gourdin et al.

Title Page

Abstract

Introduction

Conclusions

References

Tables

Figures

◀

▶

◀

▶

Back

Close

Full Screen / Esc

Printer-friendly Version

Interactive Discussion

Sources and export of particle-borne OM during a monsoon flood in a catchment of northern Laos

E. Gourdin et al.

Title Page

Abstract

Introduction

Conclusions

References

Tables

Figures

◀

▶

◀

▶

Back

Close

Full Screen / Esc

Printer-friendly Version

Interactive Discussion

et al., 2010). It also constitutes a potential vector for various contaminants such as metals, polycyclic aromatic hydrocarbons or faecal bacteria (Ribolzi et al., 2010; Gatteuille et al., 2014). In order to reduce the extent of these negative impacts, sediment delivery by rivers needs to be monitored and controlled. The design and implementation of appropriate management procedures require the identification of suspended organic matter sources and dynamics. To this end, total organic carbon (TOC) concentration measurements as well as natural $^{15}\text{N}/^{14}\text{N}$ (e.g., Mariotti et al., 1983; Kao and Liu, 2000; Huon et al., 2006) and $^{13}\text{C}/^{12}\text{C}$ (e.g., Masiello and Druffel, 2001; Hilton et al., 2010; Smith et al., 2013) stable isotope fingerprinting methods may be used on particulate material collected from hillslopes to rivers, either independently or in combination with fallout radionuclides to document variations in sediment sources and pathways across catchments (e.g., Ritchie and McCarty, 2003; Ellis et al., 2012; Schindler Wildhaber et al., 2012; Ben Slimane et al., 2013; Koiter et al., 2013). In addition, complementary information on sediment conveyed to the river by runoff and overland flow can also be inferred from water tracers such as ^{18}O natural abundance (for a review see Klaus and McDonnell, 2013).

In this study, rainwater, stream water, overland flow and suspended sediment loads were sampled in the partly cultivated headwater catchment of the Houay Xon river, a small tributary of the Mekong River in Laos, during an erosive flood event that took place at the beginning of the 2012 rainy season in order to: (1) estimate the overland flow contribution to stream water and, (2) discriminate the respective contributions of surface soil and channel or riverbed material to particulate organic matter export. This study is complementary to a previous one dedicated to the quantification of sediment dynamics during the same erosive flood event from fallout radionuclide measurements (Gourdin et al., 2014).

2 Study site

The Houay Pano catchment, part of the MSEC (Monitoring Soil Erosion Consortium) network since 1998 (Valentin et al., 2008), is located 10 km south of Luang Prabang in northern Laos (19.84° N–102.14° E; Fig. 1).

The tropical monsoon climate of the region is characterized by the succession of dry and wet seasons. Almost 80 % of annual rainfall (1960–2013 average: 1302 ± 364 mm yr⁻¹) occurs during the rainy season, from May to October (Ribolzi et al., 2008). The Houay Pano permanent stream has an average base flow of 0.4 ± 0.1 L s⁻¹ and is equipped with 5 gauging stations that subdivide the catchment into nested sub-catchments. Two of these stations, S1 and S4, draining 20 ha and 60 ha respectively, are located along the main stem of the stream. Two additional stations (S7 and S8) draining two hillslopes (0.6 ha each) connected to the main stream between S1 and S4 were also monitored. Between S1 and S4, water flows through a swamp (0.19 ha), fed by a permanent groundwater table (Fig. 1). Only temporary foot slope and flood deposits can be found along the narrow section of the stream and the swamp represents the major sediment accumulation zone in the catchment. The Houay Pano stream flows into the Houay Xon River (22.4 km² catchment) and is continuously monitored at S10 (draining a 11.6 km² sub-catchment), located 2.8 km downstream of S4. The Houay Xon is a tributary of the Nam Dong River, flowing into the Mekong River within the city of Luang Prabang (Ribolzi et al., 2010).

The geological basement of the Houay Pano catchment is mainly composed of pelites, sandstones and greywackes, overlaid in its uppermost part by Carboniferous – Permian limestone cliffs. Soils consist of deep (> 2 m) and moderately deep (> 0.5 m) Alfisols (UNESCO, 1974), except along crests and ridges where Inceptisols can be found (Chaplot et al., 2009). Native vegetation consisted of lowland forest dominated by bamboos that were first cleared to implement shifting cultivation of upland rice at the end of the 1960s (Huon et al., 2013). Elevation across the Houay Xon catchment ranges between 272 and 1300 m a.s.l. As cultivation takes place on steep slopes rang-

BGD

11, 9341–9378, 2014

Sources and export of particle-borne OM during a monsoon flood in a catchment of northern Laos

E. Gourdin et al.

Title Page

Abstract

Introduction

Conclusions

References

Tables

Figures

◀

▶

◀

▶

Back

Close

Full Screen / Esc

Printer-friendly Version

Interactive Discussion

ing between 3 and 150 %, land use evolution in the catchment is prone to soil erosion (Chaplot et al., 2005; Ribolzi et al., 2011). Due to the decline of soil productivity triggered by soil erosion over the years (Patin et al., 2012) and to an increasing labour need to control weed invasion (Dupin et al., 2009), farmers progressively replaced rice fields by teak plantations in the catchment (Fig. 1). In 2012 the Houay Pano catchment was covered by teaks (36 %), rotating cropping lands under fallow (35 %), Job's tears (10 %), bananas (4 %), upland rice (3 %) and secondary forest (< 9 %). The vegetation cover was different in the larger area drained by the Houay Xon River, with 56 % of forests, 15 % under teak plantations and 23 % croplands.

3 Materials and methods

3.1 Sample and data collection

Rainfall, stream and overland flow waters were sampled during the 23 May flood in 2012. Rainfall intensity (I) was monitored with an automatic weather station (elevation: 536 m a.s.l.; Fig. 1) and stream discharge was calculated from water level continuous recording and rating curves. Estimates of event water discharge (EWD), defined here as the total water volume exported from each subcatchment during the event minus the base flow discharge, were calculated by adding sequential water volumes corresponding to the average discharge between two water level measurements. Specific runoff (SR, in mm) was obtained by dividing EWD by the corresponding sub-catchment area (Chow et al., 1988).

Rainfall was sampled with three cumulative collectors located: in the village near the confluence between the Houay Pano and Houay Xon streams, near a teak plantation on the hillslopes located just upstream of the village and within the Houay Pano catchment (Fig. 1). The runoff coefficient (RC) corresponds to the fraction of total rainfall that was exported from the catchment during the event. Overland flow was collected at the outlet of 1 m² experimental plots (OF_{1m²}) designed for runoff studies (Patin et al., 2012). For

BGD

11, 9341–9378, 2014

Sources and export of particle-borne OM during a monsoon flood in a catchment of northern Laos

E. Gourdin et al.

Title Page

Abstract

Introduction

Conclusions

References

Tables

Figures

◀

▶

◀

▶

Back

Close

Full Screen / Esc

Printer-friendly Version

Interactive Discussion

Sources and export of particle-borne OM during a monsoon flood in a catchment of northern Laos

E. Gourdin et al.

Title Page

Abstract

Introduction

Conclusions

References

Tables

Figures

◀

▶

◀

▶

Back

Close

Full Screen / Esc

Printer-friendly Version

Interactive Discussion



one of them (Fig. 2) the evolution of rainwater, overland flow and suspended organic matter composition was monitored during a rainfall event (1 June 2012), simultaneously at its outlet and for a ca. 8 m² rain-collector set-up located a few meters apart. The experiment was conducted on a soil with 33 % slope and ca. 60 % fallow vegetation cover (ca. 10 cm high; Fig. 2a). The rain collector was installed at 1.8 m above soil surface to avoid splash contamination. Four samples were collected in the first 3 cm of a soil profile (0–5 mm; 6–10 mm; 11–20 mm; 21–30 mm) within a ca. 400 cm² area adjacent to the experimental plot to estimate the composition of organic matter in the topsoil layer (Fig. 2b).

River water was collected in polyethylene bottles for each 20 mm water level change by automatic samplers installed at each gauging station. Sixty-nine total suspended sediment (TSS) samples were collected for five stations, S1, S4 and S10 on the main stem and S7–S8 for hillslopes drained by temporary tributaries (Fig. 1). Samples were dried shortly after collection in an oven ($t \approx 100^\circ\text{C}$) for 12–48 h. To complete the topsoil data set available for the catchment (Huon et al., 2013), additional soil cores were collected on hillslopes connected to the Houay Pano stream and the Houay Xon River (Fig. 1) in May and December 2012. Sampling was further completed with several gully ($n = 5$) and riverbank ($n = 6$) samples in December 2012 to document the characteristics of the potential subsurface sources of sediment to the river.

Cumulated suspended sediment yields (SSY) were calculated at each station by adding the total suspended sediment (TSS) masses exported between two successive samples. The TSS concentration was considered to vary linearly between successive measurements. Specific sediment yields (S_Y) were calculated by dividing the cumulated SSY by the corresponding drainage area.

3.2 Particulate organic matter composition measurements

All samples were finely grounded with an agate mortar, weighed and packed into tin capsules (5 mm × 9 mm) for analysis. Total organic carbon (TOC) and total nitrogen (TN) concentrations, and ¹³C/¹²C and ¹⁵N/¹⁴N stable isotopes were measured using

the Elementar[®] VarioPyro cube analyzer on line with a Micromass[®] Isoprime Isotope Ratio Mass Spectrometer (IRMS) facility (IEES, Paris). Analytical precision was better than $\pm 0.1\%$ vs. PDB-AIR standards (Coplen et al., 1983) and 0.1 mg g^{-1} (equivalent to 0.01 wt.%) for $\delta^{13}\text{C}$ – $\delta^{15}\text{N}$ and TOC–TN, respectively. Data reproducibility was checked by replicate analyses of selected samples and of a tyrosine laboratory standard (Girardin and Mariotti, 1991). Due to the absence of carbonate minerals in sediments and suspended loads, no additional treatment was required. For the entire flood, total particulate organic carbon yields (C_{SSY}) were calculated by summing the successive TOC contents associated with suspended sediments (SSY multiplied by TOC concentration). The TOC concentration of particulate organic matter was assumed to vary linearly between successive samples. Specific TOC yields (C_Y) were calculated by dividing the cumulated C_{SSY} by the corresponding drainage area.

3.3 Water $\delta^{18}\text{O}$ and electrical conductivity measurements

Water aliquots were recovered in 30 mL glass flasks from stream, overland flow and rain samples (see Sect. 3.1 for details) and filtered using $< 0.2 \mu\text{m}$ acetate filters. Stable $^{18}\text{O}/^{16}\text{O}$ isotope measurements were carried out using the standard CO_2 equilibration method (Epstein and Mayeda, 1953) and determined with a VG Optima[®] mass spectrometer (IEES, Thiverval-Grignon). Isotopic ratios are reported using the $\delta^{18}\text{O}$ notation, relative to the Vienna-Standard Mean Ocean Water (V-SMOW; Gonfiantini, 1978) with an analytical precision better than $\pm 0.1\%$. Water electrical conductivity (EC) was monitored every 6 min at the inlet of each gauging station using Schlumberger in situ CTD probes. Additional measurements were conducted using an YSI[®] 556 probe for manually collected samples. Hydrograph separation was carried out with end-member mixing equations using water electrical conductivity and $\delta^{18}\text{O}$ measurements (Sklash and Farvolden, 1979; Ribolzi et al., 2000; Ladouche et al., 2001).

BGD

11, 9341–9378, 2014

Sources and export of particle-borne OM during a monsoon flood in a catchment of northern Laos

E. Gourdin et al.

Title Page

Abstract

Introduction

Conclusions

References

Tables

Figures

◀

▶

◀

▶

Back

Close

Full Screen / Esc

Printer-friendly Version

Interactive Discussion

4 Results

4.1 Composition of the potential sources of particulate organic matter in the catchment

The mean organic matter characteristics are reported in Table 1 for surface soils, gullies and stream banks collected in the catchment, together with ^{137}Cs activity determined on the same sample aliquots (Huon et al., 2013; Gourdin et al., 2014). In contrast to the high ^{137}Cs activities measured in surface soil samples, gully and riverbank sites are depleted in this radioisotope (Table 1).

Surface (soils) and subsurface (stream banks and gullies) sources of particulate organic matter are best discriminated by their TOC content that is higher in surface soils. The dominance of C_3 photosynthetic pathway plants across the catchment is reflected by low $\delta^{13}\text{C}$ values in soils ($-25.5 \pm 1.4\text{‰}$). However, soil-originating particles accumulated in sediments of the swamp provide ^{13}C -enriched compositions, up to ca. -15‰ , that are explained by the strong contribution of particulate organic matter derived from C_4 photosynthetic pathway plants. The latter are mainly Napier grass growing in the swamp and along limited sections of the stream channel, and to a much lower extent, Job's tears and maize cultivated on nearby hillslopes (Huon et al., 2013). Soil surface and subsurface sources can also be distinguished by their $\delta^{15}\text{N}$ values that are slightly lower for surface sources.

4.2 Monitoring water and particulate organic matter exports at the microplot scale during a rainfall event

The distribution of organic matter composition with soil depth is displayed on Fig. 2b. The TOC content decreases exponentially with depth together with TN (not plotted), leading to a nearly constant TOC:TN ratio of ca. 10 (Fig. 2b). Both $\delta^{13}\text{C}$ and $\delta^{15}\text{N}$ increase with soil depth from -26.3 to -24.7‰ and from 6.6 to 8.6‰ , respectively, reflecting the contribution of fallow vegetation debris depleted in ^{13}C and ^{15}N with respect

BGD

11, 9341–9378, 2014

Sources and export of particle-borne OM during a monsoon flood in a catchment of northern Laos

E. Gourdin et al.

Title Page

Abstract

Introduction

Conclusions

References

Tables

Figures

◀

▶

◀

▶

Back

Close

Full Screen / Esc

Printer-friendly Version

Interactive Discussion

Sources and export of particle-borne OM during a monsoon flood in a catchment of northern Laos

E. Gourdin et al.

Title Page

Abstract

Introduction

Conclusions

References

Tables

Figures

◀

▶

◀

▶

Back

Close

Full Screen / Esc

Printer-friendly Version

Interactive Discussion

to soil organic matter (Balesdent et al., 1993). Overland flow samples (OF) were collected continuously at the outlet of the experimental plot during the 1 June storm that lasted for 45 min. Cumulated rainfall was ca. 11 mm and its intensity reached 30 mm h^{-1} during 20 min. Suspended sediment concentration increased to a maximum of 4.7 g L^{-1} (Fig. 2c and d). The estimated runoff coefficient was 77 % during the entire storm with an average infiltration rate of 3.3 mm h^{-1} , assuming no evaporation during rainfall. As shown on Fig. 2c, suspended sediments exported from the experimental plot were characterized by TOC, TOC/TN, $\delta^{13}\text{C}$ and $\delta^{15}\text{N}$ values that match topsoil organic matter composition (Fig. 2b). The higher TOC and lower $\delta^{13}\text{C}$ and $\delta^{15}\text{N}$ recorded at the beginning of the storm likely result from the preferential export of vegetation debris. The evolution of rainwater and OF $\delta^{18}\text{O}$ is shown on Fig. 2d. At the beginning of the storm, both displayed a similar decreasing $\delta^{18}\text{O}$ trend (from -3.8 to -5.5 ‰) with increasing rainfall intensity, concomitant to a rise of the suspended load. Overland flow EC averaged $20 \pm 6 \mu\text{S cm}^{-1}$ (range: 15 – $36 \mu\text{S cm}^{-1}$, $n = 17$). The values are consistent with the ones of two other cumulated OF samples, 21 and $43 \mu\text{S cm}^{-1}$, collected in the Houay Pano catchment during the 23 May event (see Sect. 4.3). Contrasted increasing trends were also observed for rain- and OF- $\delta^{18}\text{O}$ contents (reaching -1.7 ‰ and -4.0 ‰, respectively) during the falling water stage. They reflected the mixing of progressively ^{18}O -enriched rainwater with former ^{18}O -depleted rainwater temporarily stored in the topsoil. It is likely that OF that triggers soil detachment and suspended sediment export will better reflect the contribution of event water to the main stream than rainwater.

4.3 Hydro-sedimentary characteristics of the 23 May flood

The 23 May flood was triggered by a 48 min storm that brought 27 mm of cumulated rainfall between 11.36 a.m. and 12.24 p.m. According to Bricquet et al. (2003), this event has a return period of ca. 0.01 year (34.7 mm day^{-1}). It was the first significant erosive event of the 2012 rainy season and the first event with rainfall intensity exceed-

ing 80 mm h^{-1} (6 min time steps). The main hydro-sedimentary characteristics of the flood are reported for the three gauging stations in Fig. 3I–IIIa–d.

The lag time between stream discharge (Q) and rainfall intensity peaks differed at the successive stations. Q increased 10 min after the rainfall peak and reached its maximum 10 min later at S1 (Fig. 3Ia), whereas both peaks were synchronous at S4 (Fig. 3IIa). Downstream, the lag time between rainfall and Q peaks increased to 70 min at S10 (Fig. 3IIIa). The evolution of TSS concentration that peaked at $24\text{--}47 \text{ g L}^{-1}$ (Fig. 3I–IIIb) displayed counterclockwise hysteresis dynamics (Williams, 1989; Lenzi and Marchi, 2000) at the three stations. Even though Q increased faster than TSS concentration at the beginning of the flood, water EC decreased concomitantly at the three stations (Fig. 3I–IIIc). This behaviour suggests the progressive mixing of pre-event water (i.e. groundwater) with a low TSS load by weakly mineralized event water (i.e. overland flow) with high sediment loads, the proportion of the latter increasing with decreasing EC. Pre-event EC values measured in the stream just before the flood were 394 , 320 and $450 \mu\text{S cm}^{-1}$ at S1, S4 and S10, respectively (Fig. 3I–IIIc) in contrast with the low values determined for OF (see above). As expected, the highest values were recorded at S10, which is located downstream of riparian villages (Ribolzi et al., 2010) where high EC wastewaters are directly released into the river. In contrast, upstream of this village, stream waters exclusively originate from cultivated lands. Pre-event water ^{18}O content was estimated to -7.1 ‰ at station S4 with samples collected before peak flow rise (Fig. 3IId). However, for S1 and S10, automatic sampling only took place during the water rising stage and the composition of pre-event water had to be estimated. At S1, a $\delta^{18}\text{O}$ value of -8 ‰ corresponding to a maximum EC of $394 \mu\text{S cm}^{-1}$ was estimated by fitting the correlative trend (see Sect. 5). Pre-event and event waters could not be distinguished with $\delta^{18}\text{O}$ signatures at S10. Overall, despite the limited number of samples collected, the composition of cumulated rainwater remained rather constant in the catchment (-5.1 , -5.5 and -5.6 ‰), averaging $-5.4 \pm 0.3 \text{ ‰}$.

Sources and export of particle-borne OM during a monsoon flood in a catchment of northern Laos

E. Gourdin et al.

Title Page

Abstract

Introduction

Conclusions

References

Tables

Figures

◀

▶

◀

▶

Back

Close

Full Screen / Esc

Printer-friendly Version

Interactive Discussion



4.4 Particulate organic matter export at catchment scales during the 23 May flood

Large variations in suspended organic matter composition were recorded at S1 with TOC concentration (20–70 mg C g⁻¹, Fig. 3Ie), TOC/TN (8–31, Fig. 3If), $\delta^{13}\text{C}$ (-26 to -15‰, Fig. 3Ig) and $\delta^{15}\text{N}$ (5.5–8.0‰, Fig. 3Ih) measurements. They all indicate changes in the source delivering suspended organic matter during the rising water stage. The $\delta^{13}\text{C}$ signature of suspended organic matter reach the average composition ($-25.5 \pm 1.4\text{‰}$; Table 1) of topsoil organic matter in the catchment at peak flow and during the recession stage (Fig. 3I–IIg). Due to larger and more heterogeneous areas drained at S4 and S10, the temporal evolution of TOC/TN, $\delta^{13}\text{C}$ and $\delta^{15}\text{N}$ in TSS (Fig. 3II–IIIe–h) were less contrasted than at S1. At S10, the mean TOC/TN was higher (17.0 ± 3.2) than at S1 (13.1 ± 5.9) and S4 (10.3 ± 0.9), reflecting a greater contribution of vegetation debris and/or weakly mineralized organic matter downstream than in upper parts of the catchment (Table A1). Furthermore, the highest TOC/TN (23; Fig. 3IIIf) was obtained during the water discharge peak at S10 whereas it was recorded at the beginning of the rising stage at S1 (31; Fig. 3If).

5 Interpretation and discussion

5.1 Overland flow contribution to stream discharge

As overland flow is the main supply of eroded particulate organic matter to the streams during the flood, hydrograph separation in pre-event groundwater and event water contributions using end-members mixing equations should provide information on water dynamics and suspended sediment sources during the flood. However, several questions may arise regarding the relevance of using water mass tracers to constrain end-members signatures and provide reliable estimates of overland flow contribution.

BGD

11, 9341–9378, 2014

Sources and export of particle-borne OM during a monsoon flood in a catchment of northern Laos

E. Gourdin et al.

Title Page

Abstract

Introduction

Conclusions

References

Tables

Figures

◀

▶

◀

▶

Back

Close

Full Screen / Esc

Printer-friendly Version

Interactive Discussion

5.1.1 Evolution of water composition during the flood

Water electrical conductivity and $\delta^{18}\text{O}$ measurements conducted on rainwater, overland flow and stream water highlight in-channel mixing processes between base flow groundwater (pre-event water) and event water characterized by contrasted signatures (Fig. 4I).

At S1 (Fig. 4Ia), all samples are aligned between the PEW and OF_{1m^2} end-members during both rising and recessing stages, suggesting that the composition of corresponding source remained constant during the event. This condition is one of the assumptions underpinning hydrograph separation procedures (e.g. Buttle, 1994; Ribolzi et al., 2000; Klaus and McDonnell, 2013). At S4 (Fig. 4Ib), the evolution of stream water composition during the flood displays a more complex pattern, with the succession of three phases characterized by distinct behaviours. During the rising stage, a similar trend between PEW and OF_{1m^2} is observed as for S1. Near peak flow, stream water EC and $\delta^{18}\text{O}$ concomitantly decrease towards the signature of cumulated rainwater samples (Fig. 4Ib) until the dilution of PEW by EW reaches its maximum. This behaviour likely reflects the progressive depletion of rainwater in ^{18}O during the storm, as observed during the microplot experiment (Fig. 2d), following a Rayleigh-type distillation process (Dansgaard, 1964). The decrease of EC in stream water is also consistent with the supply of weakly mineralized overland flow water mixing rainwater and pre-event soil water with low and high dissolved loads, respectively. A remarkable point is that the water composition supplied by S7-S8 sub-catchments, referred to as $\text{OF}_{0.6\text{ha}}$ (Fig. 4Ib), closely matches the composition of stream water during this period. Finally, during the third phase corresponding to the recession period, the composition of the river water evolved towards the “initial” PEW signature along a third mixing line. At S10, stream water composition displayed large variations in EC but limited changes in $\delta^{18}\text{O}$ (range: from -6.0 to -5.2‰ , Fig. 4Ic). The EC values, ranging between 155 and $450\ \mu\text{S cm}^{-1}$, suggest a high contribution of OF at this station.

Sources and export of particle-borne OM during a monsoon flood in a catchment of northern Laos

E. Gourdin et al.

Title Page

Abstract

Introduction

Conclusions

References

Tables

Figures

◀

▶

◀

▶

Back

Close

Full Screen / Esc

Printer-friendly Version

Interactive Discussion



5.1.2 Catchment hydrological characteristics inferred from hydrograph separation

As highlighted by Klaus and McDonnell (2013), high-frequency analyses of rainfall-runoff are necessary to record end-members intra-event signature variations and reduce uncertainties on hydrograph separation. The microplot experiment previously described recorded such temporal variations during a single storm event (Fig. 2d). The OF signature displayed lower variations (-5.5 to -3.7 ‰) than rainwater (-5.6 to -1.7 ‰) as a result of mixing between rain and soil water. Although samples could not be taken during the 23 May flood, a similar intra-storm evolution magnitude of ca. 2‰ for $OF-\delta^{18}O$ was assumed. In order to estimate event water contribution to total water discharge monitored at each station, this possible intra-storm variation of rainwater and overland flow signature must be taken into account, as suggested by McDonnell et al. (1990). The very close $\delta^{18}O$ values of the three rainwater samples collected on 23 May across the catchment remain consistent with the first assumption formulated by Harris et al. (1995) regarding spatial uniformity of cumulated rainwater isotopic signature. However, the behaviour of stream water during peak discharge at S4 (Figs. 31ld–41b) suggests the evolution of the OF end-member signature towards low $\delta^{18}O$ (as recorded for $OF_{0.6ha}$ in Fig. 41b), consistent with a Rayleigh-type distillation of rainwater. Pre-event soil water signature, likely enriched in ^{18}O by evaporation at the onset of the rainy season (e.g., Hsieh et al., 1998), could not be characterized. Its higher $\delta^{18}O$ range can be assumed to be responsible for the higher $\delta^{18}O$ observed for OF_{1m^2} during the 23 May flood (-3.9 to -2.5 ‰; Fig. 41b). The higher EC values recorded for $OF_{0.6ha}$ compared to OF_{1m^2} likely result from dissolved elements loading by runoff due to interactions between rainwater, vegetation, and soil particles along slopes. As the temporal evolution of rainwater and of the resulting $OF-\delta^{18}O$ values could not be measured during the 23 May flood, we used EC only to provide estimates of overland flow contribution, taking into account the potential variation of this end-member's signature, from 20 to $150 \mu S cm^{-1}$, during the event (Fig. 41l).

Sources and export of particle-borne OM during a monsoon flood in a catchment of northern Laos

E. Gourdin et al.

Title Page

Abstract

Introduction

Conclusions

References

Tables

Figures

◀

▶

◀

▶

Back

Close

Full Screen / Esc

Printer-friendly Version

Interactive Discussion



Estimates of event water discharge (EWD), specific runoff (SR) and runoff coefficient (RC) are summarized in Table 2.

Runoff coefficients are rather low in most parts of the catchment (4.0 and 3.9 % at S1 and S10, respectively), except at S4 which displayed a higher value of 11.7 % (Table 2).

Overall, those low runoff coefficients remained consistent with the high infiltration rates reported by Patin et al. (2012) in the same area ($> 100 \text{ mm h}^{-1}$). Chaplot and Poesen (2012) reported an annual runoff coefficient of ca. 13 % for twelve 1 m^2 plots monitored in this catchment. Values decrease both with hillslope downward position of the experimental plots and for increasing drainage area, down to 6 % for S4 and 1.5 % for S10. Estimates of the OF contribution to total water discharge, based on the evolution of water EC, are displayed on Fig. 4II. At discharge peak, OF was lower at S1 (53–80 %) than at S4 (78–100 %) and S10 (67–95 %). The highest value was obtained at S4 where the highest runoff coefficient was also recorded. This behaviour likely results from a different soil cover in this sub-catchment. Indeed, teak plantations prone to soil erosion and low infiltrability conditions (Patin et al., 2012) covered 32 % of this sub-catchment area in 2012, whereas it had a two-fold smaller extension in the drainage areas of S1 (14 %) and S10 (15 %). Moreover, the annual runoff coefficients reported by Chaplot and Poesen (2012) at S4 and S10 were lower than those reported in this study, but they were measured when teak plantations covered a much lower part of the catchment (2002–2003, Chaplot et al., 2005). Overall, it is likely that teak plantations will enhance overland flow and soil erosion at least during the years following land use conversion.

5.2 Particulate organic matter delivery

5.2.1 Sources and dynamics of suspended organic matter during the 23 May flood

Variations in the composition of particulate organic matter reflect changes in the source supplying suspended sediment in the catchment during the flood. For S1 and S4, this

BGD

11, 9341–9378, 2014

Sources and export of particle-borne OM during a monsoon flood in a catchment of northern Laos

E. Gourdin et al.

Title Page

Abstract

Introduction

Conclusions

References

Tables

Figures

◀

▶

◀

▶

Back

Close

Full Screen / Esc

Printer-friendly Version

Interactive Discussion



matter exported from cultivated fields and supplied by overland flow to the main stream (low TOC/TN, high $\delta^{15}\text{N}$). However, the occurrence of light density charcoal fragments produced by slash-and-burn might have slightly increased TOC/TN with respect to soil organic matter (Soto et al., 1995; Rumpel et al., 2006). Overland flow supply of particulate organic matter exported from soils that are currently or were previously cultivated with upland rice, is largely dominant at S4, compared to S1 (Fig. 5Ia, b and IIa, b). Fields cropped with C_4 -plants only cover small areas in the catchment and their imprint on soil organic matter composition is therefore limited (Huon et al., 2013). The $\delta^{13}\text{C}$ recorded during and after the water discharge peak were similar (-25.7‰ ; Fig. 5IIa and b) to those of surface soils, reflecting the dominance of surface vs. subsurface sources in Houay Pano catchment. At S8, located close to S4 (Fig. 1), $\delta^{15}\text{N}$ increased noticeably from 6.5 to 8.3‰ during the storm, indicating that ^{15}N -depleted organic matter (i.e., vegetation debris) was first exported and that erosion progressively affected deeper ^{15}N -enriched layers of the topsoil (Table 1). In contrast to the two other stations, the maximum TOC/TN (23) recorded downstream at S10 occurred during the water discharge peak (Figs. 3III f and 5Ic). Fresh organic matter characterized by high ratios is exported with a time lag due to the remote location of its source (Gurnell, 2007). Suspended organic matter transported at the beginning of the flood (range: from -23 to -21‰ ; Table A1, Fig. 5IIc) is enriched in ^{13}C compared to the mean surface soil ($-25.5 \pm 1.4\text{‰}$) and match subsurface soil signatures (stream banks and gullies, Table 1). This observation validates previous findings showing the dominance of riverbank erosion suggested by the depletion in fallout radionuclides measured for sediments collected at this station (Gourdin et al., 2014). Contribution of overland flow to stream water discharge derived from hydrograph separation can be linked to the source of suspended organic matter (Fig. 5III) as well as to the extent of particulate organic matter transfer (Fig. 5IV). In terms of water–sediment dynamics, high OF contributions (above ca. 50%) supply large quantities of soil organic matter (fingerprinted by low TOC contents and enriched isotopic compositions) to the river. In contrast, low OF contributions may indicate the dominance of riverbank erosion and remobilization

Sources and export of particle-borne OM during a monsoon flood in a catchment of northern Laos

E. Gourdin et al.

[Title Page](#)[Abstract](#)[Introduction](#)[Conclusions](#)[References](#)[Tables](#)[Figures](#)[◀](#)[▶](#)[◀](#)[▶](#)[Back](#)[Close](#)[Full Screen / Esc](#)[Printer-friendly Version](#)[Interactive Discussion](#)

of material deposited on the riverbed after previous floods. Based on this hydrograph separation, it is then possible to draw sediment and particulate organic carbon budgets at the catchment scale in areas where surface soil erosion dominates.

5.2.2 Suspended sediment TOC–¹³⁷Cs relationships

5 Positive correlative trends between soil TOC and ¹³⁷Cs inventories suggest that a similar process, i.e. erosion and erosion-induced carbon depletion, controlled their concomitant decrease since the onset of cultivation in the 1960s (Huon et al., 2013). Similar positive correlations were reported by Smith and Blake (2014) for riverine sediments in parts of their study sites. We could not derive such relationships for suspended sediment loads during the 23 May flood. This observation may reflect selective detachment and transport, with respect to cultivated soils, of small size mineral-bound organic matter to the rivers. It could however also result from the local contribution of channel bed organic matter, degraded with time, inducing TOC depletion and ¹³C enrichment. This later interpretation is supported by the large proportion of remobilized sediments fingerprinted by the low ⁷Be : ²¹⁰Pb_{xs} activity ratios measured in suspended sediment loads (Gourdin et al., 2014).

5.2.3 Suspended sediment and carbon delivery at catchment scale

Total suspended sediment exports are summarized in Table 3 for S1, S4 and S10 sub-catchments.

20 The sediment yield (S_Y) of ca. 433 kg ha⁻¹ at S4 is greater than at S1 and S10 (Table 3) and consistent with higher specific runoff and runoff coefficient values (Table 2). Due to the low S_Y observed at S1, the succession of nested catchments was not related to a decrease in specific delivery when drainage area increased. Compared to the 2002–2003 annual sediment deliveries at S4 (2090 kg ha⁻¹ yr⁻¹) and S10 (540 kg ha⁻¹ yr⁻¹) reported by Chaplot and Poesen (2012), the 23 May flood represents ca. 21 % of the total annual exports recorded for both stations. These deliveries

BGD

11, 9341–9378, 2014

Sources and export of particle-borne OM during a monsoon flood in a catchment of northern Laos

E. Gourdin et al.

Title Page

Abstract

Introduction

Conclusions

References

Tables

Figures

◀

▶

◀

▶

Back

Close

Full Screen / Esc

Printer-friendly Version

Interactive Discussion

are very high for a single event of moderate intensity. However, fallout radionuclide measurements (Gourdin et al., 2014) indicate that the 23 May flood was the first important erosive event of the 2012 rainy season and that exported matter mainly consisted of remobilized river channel sediments (ca. 80 %) that may not have been fully taken into account in the previous study.

Carbon specific deliveries (C_Y) suggest a higher erodibility of the S4 draining area, exporting ca. 8.3 kg C ha^{-1} of soil organic carbon, i.e. more than twice the quantity exported from S1 and S10 ($2.9\text{--}3.7 \text{ kg C ha}^{-1}$; Table 3). This behaviour may be related to higher RC (11.7 %; Table 2) and OF contribution at discharge peak (78–100 %; Fig. 4IIb) estimated at this station. As for sediment delivery, we calculated a much higher carbon flux exported by the catchment than previously reported by Chaplot and Poesen (2012), i.e., 8.5 and $1.4 \text{ kg C ha}^{-1} \text{ yr}^{-1}$ for S4 and S10, respectively. To the best of our knowledge, this discrepancy may be explained by the different TOC concentrations used for carbon flux calculation in both studies. In this study the values are almost 5-fold higher for S4 (25 vs. 4.1 mg C g^{-1}) and 14-fold higher for S10 (36 vs. 2.6 mg C g^{-1}). As the same analytical method was used in both studies, these differences could also be explained by a greater contribution of deep soil layers through linear erosion (gullies and riverbanks) during the 2002 rainy season, responsible for the export of sediments with low TOC content ($< 5 \text{ mg C g}^{-1}$) in all catchments draining a surface exceeding 0.6 ha . Total organic carbon and total nitrogen concentrations of riverine sediments are usually higher than in soils due to preferential mobilisation and transport of fine and light soil organic fractions after aggregates destruction (Stoltenberg and White, 1953). However, Chaplot and Poesen (2012) observed rather similar TOC enrichment factors (close to 1), suggesting a good stability of soil aggregates in their study. The low carbon yields (8.5 and $1.4 \text{ kg C ha}^{-1} \text{ yr}^{-1}$, for S4 and S10 respectively) reported by these authors indicate that nearly all soil particulate organic matter deposited on hillslopes before reaching the river channel. The connectivity of hillslopes to the stream channel may also have changed since 2002–2003 due to the replacement of cultivated plots by teak plantations initiated in 2009 in the catchment.

Sources and export of particle-borne OM during a monsoon flood in a catchment of northern Laos

E. Gourdin et al.

Title Page

Abstract

Introduction

Conclusions

References

Tables

Figures

◀

▶

◀

▶

Back

Close

Full Screen / Esc

Printer-friendly Version

Interactive Discussion



Teaks are characterized by large leaves that concentrate rainwater and enhance rain-drop erosivity, soil crusting and runoff, especially after 10 years (Patin et al., 2012). However, their impact on soil erosion and organic matter export is still poorly understood (C. Valentin, personal communication, 2014) and should be further investigated.

6 Concluding remarks

The composition of suspended organic matter and stream water monitored during the first erosive event of the 2012 rainy season in a cultivated catchment of northern Laos provided an efficient way to quantify the evolution of particulate organic matter sources along a network of nested gauging stations.

In upper parts of the catchment, suspended organic matter exported was mainly originating from in-channel and nearby sources during the rising stage, and from cultivated surface soils at peak flow and during the recessing stage.

Downstream, the composition of suspended and deposited organic matter reflected the dominant supply of subsurface sources and a subsequent dilution of the soil-derived organic matter delivery by channel–bank mixing and remobilization processes.

The results of this study suggest that relationships between water flow and suspended sediment load and hydrograph separation at the outlet of catchments would be better constrained using high-resolution monitoring of overland flow than rainfall.

Finally, as higher suspended organic matter exports than in previous studies were determined, these results indicate that both the sampling period, at the onset of the rainy season (following field clearing by slash and burn in this study), and the impact of land use change played a key role for sediment delivery at the outlet of the catchment.

Acknowledgements. The authors would like to thank the Lao NAFRI (National Agriculture and Forestry Research Institute in Vientiane) and the MSEC project (Multi-Scale Environment Changes) for their support. They are also grateful to Keo Oudone Latsachack, Bounsamai Soulleuth and Chanthamousone Thammahacksa for their help in the field, to Véronique Vaury (iEES-Paris) for organic matter composition measurements, and to Patricia Richard (iEES-

Sources and export of particle-borne OM during a monsoon flood in a catchment of northern Laos

E. Gourdin et al.

Title Page

Abstract

Introduction

Conclusions

References

Tables

Figures

◀

▶

◀

▶

Back

Close

Full Screen / Esc

Printer-friendly Version

Interactive Discussion



Thiverval Grignon) for $\delta^{18}\text{O}$ measurements of water samples. Elian Gourdin received a Ph.D. fellowship from Paris-Sud University, Orsay, France. This work received financial support from the French CNRS EC2CO/BIOHEFECT program (Belcrue project).

References

- 5 Balesdent, J., Girardin, C., and Mariotti, A.: Site-related $\delta^{13}\text{C}$ of tree leaves and soil organic matter in a temperate forest, *Ecology*, 74, 1713–1721, 1993.
- Bellanger, B., Huon, S., Velasquez, F., Vallès, V., Girardin, C., and Mariotti, A.: Monitoring soil organic carbon erosion with $\delta^{13}\text{C}$ and $\delta^{15}\text{N}$ on experimental field plots in the Venezuelan Andes, *Catena*, 58, 125–150, 2004.
- 10 Ben Slimane, A., Raclot, D., Evrard, O., Sanaa, M., Lefèvre, I., Ahmadi, M., Tounsi, M., Rumpel, C., Ben Mammou, A., and Le Bissonnais, Y.: Fingerprinting sediment sources in the outlet reservoir of a hilly cultivated catchment in Tunisia, *J. Soil. Sediment.*, 13, 801–815, 2013.
- Bricquet, J.-P., Boonsaner, A., Bouahom, B., and Toan, T. D.: Statistical analysis of long series rainfall data: a regional study in South-East Asia, in: *From Soil Research to Land and Water Management: Harmonizing People and Nature*, Magliano, A. R., Valentin, C., and Penning de Vries, F., Proceedings of the IWMI-ADB Project Annual Meeting and 7th MSEC Assembly, IWMI-ADB Project Annual Meeting; MSEC Assembly, Vientiane, Lao, 7, 83–89, 2003.
- 15 Buttle, J. M.: Isotope hydrograph separations and rapid delivery of pre-event water from drainage basins, *Prog. Phys. Geog.*, 18, 16–41, 1994.
- Chaplot, V. and Poesen, J.: Sediment, soil organic carbon and runoff delivery at various spatial scales, *Catena*, 88, 46–56, 2012.
- Chaplot, V., Coadoubrozec, E., Silvera, N., and Valentin, C.: Spatial and temporal assessment of linear erosion in catchments under sloping lands of northern Laos, *Catena*, 63, 167–184, 2005.
- 25 Chaplot, V., Podwojewski, P., Phachomphon, K., and Valentin, C.: Soil erosion impact on soil organic carbon spatial variability on steep tropical slopes, *Soil Sci. Soc. Am. J.*, 73, 769, 2009.
- Chow, V. T., Maidment, D. R., and Mays, L. W.: *Applied Hydrology*, McGraw Hill Book Co., 572 pp., 1988.
- 30

Sources and export of particle-borne OM during a monsoon flood in a catchment of northern Laos

E. Gourdin et al.

[Title Page](#)

[Abstract](#)

[Introduction](#)

[Conclusions](#)

[References](#)

[Tables](#)

[Figures](#)

[⏪](#)

[⏩](#)

[◀](#)

[▶](#)

[Back](#)

[Close](#)

[Full Screen / Esc](#)

[Printer-friendly Version](#)

[Interactive Discussion](#)



Sources and export of particle-borne OM during a monsoon flood in a catchment of northern Laos

E. Gourdin et al.

[Title Page](#)

[Abstract](#)

[Introduction](#)

[Conclusions](#)

[References](#)

[Tables](#)

[Figures](#)

[◀](#)

[▶](#)

[◀](#)

[▶](#)

[Back](#)

[Close](#)

[Full Screen / Esc](#)

[Printer-friendly Version](#)

[Interactive Discussion](#)

- Copard, Y., Amiotte-Suchet, P., and Di-Giovanni, C.: Storage and release of fossil organic carbon related to weathering of sedimentary rocks, *Earth Planet. Sc. Lett.*, 258, 345–357, 2007.
- Coplen, T. B., Kendall, C., and Hopple, J.: Comparison of stable isotope reference samples, *Nature*, 302, 236–238, 1983.
- 5 Dansgaard, W.: Stable isotopes in precipitation, *Tellus*, 16, 436–468, 1964.
- Degens, E. T., Kempe, S., and Richey, J. E. (Eds.): Summary, in: *Biogeochemistry of Major World Rivers*, SCOPE Rep. 42, John Wiley and Sons, Chichester, 323–347, 1991.
- Descroix, L., González Barrios, J. L., Viramontes, D., Poulenard, J., Anaya, E., Esteves, M., and Estrada, J.: Gully and sheet erosion on subtropical mountain slopes: their respective roles and the scale effect, *Catena*, 72, 325–339, 2008.
- 10 Dixon, R. K., Brown, S., Houghton, R. A., Solomon, A. M., Trexler, M. C., and Wisniewski, J.: Carbon pools and flux of global forest ecosystems, *Science*, 263, 185–191, 1994.
- Downing, J. A., Cole, J. J., Middelburg, J. J., Striegl, R. G., Duarte, C. M., Kortelainen, P., Prairie, Y. T., and Laube, K. A.: Sediment organic carbon burial in agriculturally eutrophic impoundments over the last century, *Global Biogeochem. Cy.*, 22, 1–10, 2008.
- 15 Dupin, B., de Rouw, A., Phantahvong, K. B., and Valentin, C.: Assessment of tillage erosion rates on steep slopes in northern Laos, *Soil Till. Res.*, 103, 119–126, 2009.
- Duvert, C., Gratiot, N., Evrard, O., Navratil, O., Némery, J., Prat, C., and Esteves, M.: Drivers of erosion and suspended sediment transport in three headwater catchments of the Mexican Central Highlands, *Geomorphology*, 123, 243–256, 2010.
- Ellis, E. E., Keil, R. G., Ingalls, A. E., Richey, J. E., and Alin, S. R.: Seasonal variability in the sources of particulate organic matter of the Mekong River as discerned by elemental and lignin analyses, *J. Geophys. Res.*, 117, G01038, doi:10.1029/2011JG001816, 2012.
- 20 Epstein, S. and Mayeda, T.: Variation of ^{18}O content of waters from natural sources, *Geochim. Cosmochim. Ac.*, 4, 213–224, 1953.
- Evrard, O., Némery, J., Gratiot, N., Duvert, C., Ayrault, S., Lefèvre, I., Poulenard, J., Prat, C., Bonté, P., and Esteves, M.: Sediment dynamics during the rainy season in tropical highland catchments of central Mexico using fallout radionuclides, *Geomorphology*, 124, 42–54, 2010.
- FAO/UNEP: Tropical Forest Resources Assessment Project, FAO, Rome, 1981.
- 30 Gateuille, D., Evrard, O., Lefèvre, I., Moreau-Guigon, E., Alliot, F., Chevreuril, M., and Mouchel, J.-M.: Mass balance and depollution times of Polycyclic Aromatic Hydrocarbons in rural nested catchments of an early industrialized region (Orgeval River, Seine River basin, France), *Sci. Total Environ.*, 470–471, 608–617, 2014.

Sources and export of particle-borne OM during a monsoon flood in a catchment of northern Laos

E. Gourdin et al.

[Title Page](#)

[Abstract](#)

[Introduction](#)

[Conclusions](#)

[References](#)

[Tables](#)

[Figures](#)

[⏪](#)

[⏩](#)

[◀](#)

[▶](#)

[Back](#)

[Close](#)

[Full Screen / Esc](#)

[Printer-friendly Version](#)

[Interactive Discussion](#)



- Girardin, C. and Mariotti, A.: Analyse isotopique du ^{13}C en abondance naturelle un système automatique avec robot préparateur, *Cah. Orstom, sér. Pédol.*, XXVI, 371–380, 1991.
- Goldsmith, S. T., Carey, A. E., Lyons, W. B., Kao, S.-J., Lee, T.-Y., and Chen, J.: Extreme storm events, landscape denudation, and carbon sequestration: typhoon Mindulle, Choshui River, Taiwan, *Geology*, 36, 483–486, 2008.
- Gonfiantini, R.: Standards for stable isotope measurements in natural compounds, *Nature*, 271, 534–536, 1978.
- Gourdin, E., Evrard, O., Huon, S., Lefèvre, I., Ribolzi, O., Reyss, J.-L., Sengtaheuanghoung, O., and Ayrault, S.: Suspended sediment dynamics in a Southeast Asian mountainous catchment: combining river monitoring and fallout radionuclide analyses, *J. Hydrol.*, under review, 2014.
- Graz, Y., Di-Giovanni, C., Copard, Y., Mathys, N., Cras, A., and Marc, V.: Annual fossil organic carbon delivery due to mechanical and chemical weathering of marly badlands areas, *Earth Surf. Proc. Land.*, 37, 1263–1271, 2012.
- Gurnell, A. M.: Analogies between mineral sediment and vegetative particle dynamics in fluvial systems, *Geomorphology*, 89, 9–22, 2007.
- Harris, D. M., McDonnell, J. J., and Rodhe, A.: Hydrograph separation using continuous open system isotope mixing, *Water Resour. Res.*, 31, 157–171, 1995.
- Hilton, R. G., Galy, A., Hovius, N., Horng, M.-J., and Chen, H.: The isotopic composition of particulate organic carbon in mountain rivers of Taiwan, *Geochim. Cosmochim. Ac.*, 74, 3164–3181, 2010.
- Houghton, R. A.: Tropical deforestation and atmospheric carbon dioxide, *Clim. Change*, 19, 99–118, 1991.
- Hsieh, J. C. C., Chadwick, O. A., Kelly, E. F., and Savin, S. M.: Oxygen isotopic composition of soil water: quantifying evaporation and transpiration, *Geoderma*, 82, 269–293, 1998.
- Huang, T.-H., Fu, Y.-H., Pan, P.-Y., and Chen, C.-T. A.: Fluvial carbon fluxes in tropical rivers, *Curr. Opin. Environ. Sustain.*, 4, 162–169, 2012.
- Huon, S., Bellanger, B., Bonté, P., Sogon, S., Podwojewski, P., Girardin, C., Valentin, C., De Rouw, A., Velasquez, F., Bricquet, J.-P., and Mariotti, A.: Monitoring soil organic carbon erosion with isotopic tracers: two case studies on cultivated tropical catchments with steep slopes (Laos, Venezuela), in: *Advances in Soil Science. Soil Erosion and Carbon Dynamics*, edited by: Roose, E., Lal, R., Barthès, B., Feller, C., and Stewart, B. A., CRC Press, Boca Raton, Florida, USA, 301–328, 2006.

Sources and export of particle-borne OM during a monsoon flood in a catchment of northern Laos

E. Gourdin et al.

[Title Page](#)

[Abstract](#)

[Introduction](#)

[Conclusions](#)

[References](#)

[Tables](#)

[Figures](#)

[◀](#)

[▶](#)

[◀](#)

[▶](#)

[Back](#)

[Close](#)

[Full Screen / Esc](#)

[Printer-friendly Version](#)

[Interactive Discussion](#)

Huon, S., de Rouw, A., Bonté, P., Robain, H., Valentin, C., Lefèvre, I., Girardin, C., Le Troquer, Y., Podwojewski, P., and Sengtaheuanghoung, O.: Long-term soil carbon loss and accumulation in a catchment following the conversion of forest to arable land in northern Laos, *Agr. Ecosyst. Environ.*, 169, 43–57, 2013.

5 Kao, S. J. and Liu, K. K.: Fluxes of dissolved and nonfossil particulate organic carbon from an Oceania small river (Lanyang Hsi) in Taiwan, *Biogeochemistry*, 39, 255–269, 1997.

Kao, S. J. and Liu, K. K.: Stable carbon and nitrogen isotope systematics in a human-disturbed watershed (Lanyang-Hsi) in Taiwan and the estimation of biogenic particulate organic carbon and nitrogen fluxes, *Global Biogeochem. Cy.*, 14, 189–198, 2000.

10 Klaus, J. and McDonnell, J. J.: Hydrograph separation using stable isotopes: review and evaluation, *J. Hydrol.*, 505, 47–64, 2013.

Koiter, A. J., Owens, P. N., Petticrew, E. L., and Lobb, D. A.: The behavioural characteristics of sediment properties and their implications for sediment fingerprinting as an approach for identifying sediment sources in river basins, *Earth-Sci. Rev.*, 125, 24–42, 2013.

15 Ladouche, B., Probst, A., Viville, D., Idir, S., Baqué, D., Loubet, M., Probst, J.-L., and Bariac, T.: Hydrograph separation using isotopic, chemical and hydrological approaches (Strengbach catchment, France), *J. Hydrol.*, 242, 255–274, 2001.

Lal, R.: Soil erosion and the global carbon budget, *Environ. Int.*, 29, 437–450, 2003.

20 Lenzi, M. A. and Marchi, L.: Suspended sediment load during floods in a small stream of the Dolomites (Northeastern Italy), *Catena*, 39, 267–282, 2000.

Ludwig, W., Probst, J., and Kempe, S.: Predicting the oceanic input of organic carbon by continental erosion, *Global Biogeochem. Cy.*, 10, 23–41, 1996.

Mariotti, A., Lancelot, C., and Billen, G.: Natural isotopic composition of nitrogen as a tracer of origin for suspended organic matter in the Scheldt estuary, *Geochim. Cosmochim. Ac.*, 48, 549–555, 1983.

25 Masiello, C. A. and Druffel, E. R. M.: Carbon isotope geochemistry of the Santa Clara River, *Global Biogeochem. Cy.*, 15, 407–416, 2001.

McDonnell, J. J., Bonell, M., Stewart, M. K., and Pearce, A. J.: Deuterium variations in storm rainfall: implications for stream hydrograph separation, *Water Resour. Res.*, 26, 455–458, 1990.

30 Meybeck, M.: Riverine transport of atmospheric carbon: sources, global typology and budget, *Water Air Soil Poll.*, 70, 443–463, 1993.

Sources and export of particle-borne OM during a monsoon flood in a catchment of northern Laos

E. Gourdin et al.

[Title Page](#)

[Abstract](#)

[Introduction](#)

[Conclusions](#)

[References](#)

[Tables](#)

[Figures](#)

[◀](#)

[▶](#)

[◀](#)

[▶](#)

[Back](#)

[Close](#)

[Full Screen / Esc](#)

[Printer-friendly Version](#)

[Interactive Discussion](#)

- Schindler Wildhaber, Y., Liechti, R., and Alewell, C.: Organic matter dynamics and stable isotope signature as tracers of the sources of suspended sediment, *Biogeosciences*, 9, 1985–1996, doi:10.5194/bg-9-1985-2012, 2012.
- Sklash, M. G. and Farvolden, R. N.: The role of groundwater in storm runoff, *J. Hydrol.*, 43, 45–65, 1979.
- Smith, H. G. and Blake, W. H.: Sediment fingerprinting in agricultural catchments: a critical re-examination of source discrimination and data corrections, *Geomorphology*, 204, 177–191, 2014.
- Smith, J. C., Galy, A., Hovius, N., Tye, A. M., Turowski, J. M., and Schleppe, P.: Runoff-driven export of particulate organic carbon from soil in temperate forested uplands, *Earth Planet. Sc. Lett.*, 365, 198–208, 2013.
- Soto, B., Basanta, R., Perez, R., and Diaz-Fierros, F.: An experimental study of the influence of traditional slash-and-burn practices on soil erosion, *Catena*, 24, 13–23, 1995.
- Stoltenberg, N. L. and White, J. L.: Selective loss of plant nutrients by erosion, *Soil Sci. Soc. Am. J.*, 17, 406–410, 1953.
- Syvitski, J. P. M., Vörösmarty, C. J., Kettner, A. J., and Green, P.: Impact of humans on the flux of terrestrial sediment to the global coastal ocean, *Science*, 308, 376–380, 2005.
- Tanik, A., Beler Baykal, B., and Gonenc, I. E.: The impact of agricultural pollutants in six drinking water reservoirs, *Water Sci. Technol.*, 40, 11–17, 1999.
- Thothong, W., Huon, S., Janeau, J.-L., Boosaner, A., de Rouw, A., Planchon, O., Bardoux, G., and Parkpian, P.: Impact of land use change and rainfall on sediment and carbon accumulation in a water reservoir of North Thailand, *Agr. Ecosyst. Environ.*, 140, 521–533, 2011.
- UNESCO (United Nations Educational Scientific and Cultural Organization): *FAO/UNESCO Soil map of the world, 1 : 5,000,000, vol. 1*, UNESCO, Paris, 1974.
- Valentin, C., Agus, F., Alamban, R., Boosaner, A., Bricquet, J. P., Chaplot, V., de Guzman, T., de Rouw, A., Janeau, J. L., Orange, D., Phachomphonh, K., Podwojewski, P., Ribolzi, O., Silvera, N., Subagyono, K., Thiébaux, J. P., and Vadari, T.: Runoff and sediment losses from 27 upland catchments in Southeast Asia: impact of rapid land use changes and conservation practices, *Agr. Ecosyst. Environ.*, 128, 225–238, 2008.
- Williams, G. P.: Sediment concentration versus water discharge during single hydrologic events in rivers, *J. Hydrol.*, 111, 89–106, 1989.

Zech, W., Senesi, N., Guggenberger, G., Kaiser, K., Lehmann, J., Miano, T. M., Miltner, A., and Schroth, G.: Factors controlling humification and mineralization of soil organic matter in the tropics, *Geoderma*, 79, 117–161, 1997.

BGD

11, 9341–9378, 2014

Sources and export of particle-borne OM during a monsoon flood in a catchment of northern Laos

E. Gourdin et al.

Title Page

Abstract

Introduction

Conclusions

References

Tables

Figures



Back

Close

Full Screen / Esc

Printer-friendly Version

Interactive Discussion



Sources and export of particle-borne OM during a monsoon flood in a catchment of northern Laos

E. Gourdin et al.

Table 1. Mean organic matter composition and ^{137}Cs activity (± 1 standard deviation) for surface soils ($n = 64$), gullies ($n = 5$) and stream bank ($n = 6$) samples in the Houay Pano and Houay Xon catchments. For ^{137}Cs activity measurements, see Gourdin et al. (2014).

| Location | TOC (mg C g^{-1}) | TN (mg N g^{-1}) | TOC/TN | $\delta^{13}\text{C}$ (‰) | $\delta^{15}\text{N}$ (‰) | ^{137}Cs (Bq kg^{-1}) |
|----------------------------|---------------------------------|--------------------------------|----------------|------------------------------|------------------------------|--|
| Surface soils ^a | 25 ± 5 | 2.1 ± 0.5 | 11.6 ± 2.0 | -25.5 ± 1.4 | 6.7 ± 1.3 | 2.2 ± 0.9 |
| Stream banks ^b | 13 ± 6 | 1.1 ± 0.3 | 12.4 ± 7.7 | -23.2 ± 4.4 | 8.6 ± 1.9 | 0.4 ± 0.3 |
| Gullies ^b | 14 ± 7 | 1.4 ± 0.6 | 9.6 ± 0.8 | -22.7 ± 0.8 | 8.7 ± 2.1 | 0.4 ± 0.3 |

^a Data from Huon et al. (2013) and this study (2012).

^b This study (2012).

Title Page

Abstract

Introduction

Conclusions

References

Tables

Figures

◀

▶

◀

▶

Back

Close

Full Screen / Esc

Printer-friendly Version

Interactive Discussion

Sources and export of particle-borne OM during a monsoon flood in a catchment of northern Laos

E. Gourdin et al.

Table 2. Estimates of event water discharge (EWD) and related specific runoff (SR) and runoff coefficient (RC) for the three stations during the 23 May flood.

| Station | Drainage area (km ²) | EWD ^a (× 10 ⁶ L) | SR ^b (mm) | RC ^c (%) |
|---------|----------------------------------|--|----------------------|---------------------|
| S1 | 0.2 | 0.215 | 1.1 | 4.0 |
| S4 | 0.6 | 1.88 | 3.2 | 11.7 |
| S10 | 11.6 | 12.2 | 1.1 | 3.9 |

^a EWD = total water discharge minus baseflow discharge.

^b SR = EWD/drainage area.

^c RC = 100 × (SR/rainfall) assuming an homogeneous cumulative rainfall of 27 mm.

Title Page

Abstract

Introduction

Conclusions

References

Tables

Figures

◀

▶

◀

▶

Back

Close

Full Screen / Esc

Printer-friendly Version

Interactive Discussion

Sources and export of particle-borne OM during a monsoon flood in a catchment of northern Laos

E. Gourdin et al.

Title Page

Abstract

Introduction

Conclusions

References

Tables

Figures

◀

▶

◀

▶

Back

Close

Full Screen / Esc

Printer-friendly Version

Interactive Discussion

Table 3. Total suspended sediment yield (SSY), total particulate organic carbon yield (C_{SSY}), specific total suspended sediment yield (S_Y) and specific total organic carbon yield (C_Y) for the 23 May flood.

| Station | SSY (Mg) | C_{SSY} (kg) | S_Y^a (kg ha ⁻¹) | C_Y^b (kg C ha ⁻¹) |
|---------|-------------|-------------------|-----------------------------------|-------------------------------------|
| S1 | 2.3 | 58 | 115 | 2.9 |
| S4 | 26 | 496 | 433 | 8.3 |
| S10 | 130 | 4346 | 112 | 3.7 |

^a $S_Y = 10 \times SSY / \text{drainage area}$ in Table 2.

^b $C_Y = 10^{-2} \times C_{SSY} / \text{drainage area}$ in Table 2.

Sources and export of particle-borne OM during a monsoon flood in a catchment of northern Laos

E. Gourdin et al.

Title Page

Abstract

Introduction

Conclusions

References

Tables

Figures

◀

▶

◀

▶

Back

Close

Full Screen / Esc

Printer-friendly Version

Interactive Discussion

Table A1. Summary of data for stations S1, S4 and S10 during the 23 May flood.

| Label | Time ^a (hh:mm) | TSS ^a (g L ⁻¹) | Q ^a (L s ⁻¹) | EC ^a (μS cm ⁻¹) | δ ¹⁸ O ^a (‰ vs. V-SMOW) | TOC ^a (mg C g ⁻¹) | TN ^a (mg N g ⁻¹) | TOC/TN ^a | δ ¹³ C ^a (‰ vs. PDB) | δ ¹⁵ N ^a (‰ vs. AIR) |
|-----------------------|------------------------------|--|--|---|--|---|--|---------------------|---|---|
| Station S1 | | | | | | | | | | |
| LS0101 | 12:08 | 0.86 | 5 | 335 | -7.2 | 42.0 | 2.0 | 20.5 | -15.3 | 7.1 |
| LS0102 | 12:09 | 0.56 | 7 | 317 | -7.1 | 60.3 | 2.6 | 23.1 | -19.0 | 5.5 |
| LS0103 | 12:09 | 0.53 | 10 | 317 | -7.0 | - | - | - | - | - |
| LS0104 | 12:10 | 0.61 | 13 | 299 | -6.8 | 66.2 | 2.1 | 31.0 | -19.7 | 7.0 |
| LS0105 | 12:10 | - | 16 | 299 | - | - | - | - | - | - |
| LS0106 | 12:11 | 1.23 | 21 | 282 | -6.9 | 32.2 | 2.3 | 14.0 | -23.0 | 6.0 |
| LS0107 | 12:13 | 1.70 | 27 | 262 | -6.6 | 26.2 | 2.0 | 13.0 | -23.7 | 6.6 |
| LS0108 | 12:14 | 2.37 | 34 | 259 | -6.2 | 25.0 | 2.0 | 12.7 | -22.4 | 6.8 |
| LS0109 | 12:19 | 3.65 | 40 | 241 | -6.0 | 23.1 | 2.1 | 10.8 | -24.4 | 7.2 |
| LS0110 | 12:20 | 4.17 | 55 | 233 | -6.1 | 23.4 | 2.2 | 10.7 | -24.5 | 7.3 |
| LS0111 | 12:21 | 4.65 | 76 | 224 | -5.9 | 22.5 | 2.0 | 11.1 | -24.1 | 7.5 |
| LS0112 | 12:21 | 18.74 | 90 | 215 | -5.8 | 27.4 | 2.0 | 11.1 | -25.6 | 6.8 |
| LS0113 | 12:30 | 29.98 | 68 | 184 | -5.8 | 25.7 | 2.1 | 11.0 | -25.8 | 6.8 |
| LS0114 | 12:33 | 23.02 | 51 | 188 | -5.5 | 25.8 | 2.2 | 10.7 | -25.9 | 7.5 |
| LS0115 | 12:37 | 24.05 | 38 | 194 | -5.4 | 23.3 | 2.0 | 10.1 | -25.8 | 7.5 |
| LS0116 | 12:43 | 17.67 | 27 | 205 | -5.6 | 20.8 | 2.5 | 9.8 | -25.6 | 7.7 |
| LS0117 | 12:50 | 16.38 | 18 | 218 | -5.7 | 19.3 | 2.3 | 9.0 | -25.3 | 7.8 |
| LS0118 | 12:57 | 9.13 | 14 | 232 | -5.8 | 18.7 | 2.4 | 9.0 | -25.0 | 7.5 |
| LS0119 | 12:58 | 14.37 | 13 | 233 | -6.1 | 18.6 | 2.3 | 9.1 | -25.1 | 7.2 |
| LS0120 | 13:15 | 4.50 | 8 | 262 | -6.2 | 19.3 | 2.1 | 9.6 | -23.8 | 7.1 |
| Station S4 | | | | | | | | | | |
| LS0403 | 11:57 | 1.53 | 15 | 297 | -6.9 | - | - | - | - | - |
| LS0404 | 11:58 | 1.21 | 24 | 306 | -6.7 | - | - | - | - | - |
| LS0403-4 ^b | - | - | - | - | - | 27.7 | 2.6 | 10.8 | -23.8 | 7.1 |
| LS0405 | 12:00 | 1.16 | 33 | 306 | -6.5 | 29.9 | 2.9 | 10.4 | -23.5 | 6.5 |
| LS0406 | 12:01 | 2.71 | 42 | 262 | -6.1 | 24.8 | 2.4 | 10.2 | -24.4 | 7.2 |
| LS0407 | 12:04 | 5.83 | 54 | 216 | -5.5 | 22.6 | 2.2 | 10.5 | -25.0 | 7.2 |
| LS0408 | 12:05 | 6.83 | 76 | 205 | -5.2 | - | - | - | - | - |
| LS0409 | 12:06 | 7.25 | 114 | 198 | -5.3 | - | - | - | - | - |
| LS0408-9 ^b | - | - | - | - | - | 21.2 | 2.1 | 10.1 | -25.0 | 7.5 |
| LS0410 | 12:07 | 10.07 | 144 | 177 | -4.7 | 22.1 | 2.1 | 10.7 | -25.2 | 7.6 |
| LS0411 | 12:07 | 11.89 | 185 | 161 | -4.7 | 20.8 | 2.0 | 10.3 | -25.2 | 7.6 |
| LS0412 | 12:08 | 15.75 | 280 | 138 | -4.5 | 19.2 | 1.9 | 9.9 | -25.6 | 7.6 |
| LS0413 | 12:09 | 20.05 | 309 | 121 | -4.9 | - | - | - | - | - |
| LS0414 | 12:10 | 31.56 | 358 | 99 | -5.1 | 19.6 | 2.1 | 9.6 | -25.4 | 8.0 |

Sources and export of particle-borne OM during a monsoon flood in a catchment of northern Laos

E. Gourdin et al.

Table A1. Continued.

| Label | Time ^a (hh:mm) | TSS ^a (g L ⁻¹) | Q ^a (L s ⁻¹) | EC ^a ($\mu\text{S cm}^{-1}$) | $\delta^{18}\text{O}^a$ (‰ vs. V-SMOW) | TOC ^a (mg C g ⁻¹) | TN ^a (mg N g ⁻¹) | TOC/TN ^a | $\delta^{13}\text{C}^a$ (‰ vs. PDB) | $\delta^{15}\text{N}^a$ (‰ vs. AIR) |
|------------------------|------------------------------|--|--|--|---|---|--|---------------------|--|--|
| LS0415 | 12:11 | 46.51 | 440 | 87 | -5.2 | 21.1 | 2.1 | 10.0 | -25.6 | 7.5 |
| LS0416 | 12:20 | 28.40 | 335 | 103 | -5.4 | 24.5 | 2.1 | 11.5 | -26.0 | 7.1 |
| LS0417 | 12:23 | 23.00 | 277 | 105 | -5.4 | 24.7 | 2.2 | 11.4 | -25.8 | 7.2 |
| LS0418 | 12:26 | 17.76 | 228 | 117 | -5.6 | 24.7 | 2.1 | 11.8 | -26.0 | 7.4 |
| LS0419 | 12:34 | 11.70 | 183 | 152 | -5.6 | - | - | - | - | - |
| LS0420 | 13:20 | 12.62 | 145 | 164 | -5.6 | - | - | - | - | - |
| LS0419-20 ^b | - | - | - | - | - | 22.5 | 2.0 | 11.0 | -25.8 | 7.4 |
| LS0421 | 13:32 | 7.71 | 112 | 192 | -5.8 | 19.0 | 1.9 | 9.8 | -25.6 | 7.7 |
| LS0422 | 13:46 | 6.92 | 84 | 201 | -6.1 | 19.6 | 2.0 | 9.8 | -25.6 | 7.7 |
| LS0423 | 14:05 | 6.93 | 59 | 203 | -6.0 | - | - | - | - | - |
| LS0424 | 14:43 | 5.89 | 39 | 214 | -6.2 | - | - | - | - | - |
| LS0425 | 15:46 | 3.37 | 23 | 230 | -6.2 | - | - | - | - | - |
| LS0423-25 ^b | - | - | - | - | - | 20.9 | 2.2 | 9.6 | -25.5 | 7.3 |
| Station S10 | | | | | | | | | | |
| LS1002 | 12:24 | 7.94 | 204 | 227 | -5.5 | - | - | - | - | - |
| LS1003 | 12:28 | 5.57 | 455 | 220 | -5.5 | - | - | - | - | - |
| LS1002-3 ^b | - | - | - | - | - | 39 | 2.0 | 19.8 | -21.2 | 8.2 |
| LS1004 | 12:31 | 8.77 | 623 | 215 | -5.9 | - | - | - | - | - |
| LS1005 | 13:03 | 11.10 | 943 | 167.5 | -5.6 | - | - | - | - | - |
| LS1004-5 ^b | - | - | - | - | - | 36 | 1.9 | 19.1 | -22.6 | 7.4 |
| LS1006 | 13:06 | 23.63 | 990 | 167 | -5.7 | 44 | 1.9 | 23.1 | -21.8 | 7.0 |
| LS1007 | 13:27 | 17.02 | 1535 | 156 | -5.4 | 44 | 2.0 | 22.2 | -22.3 | 7.5 |
| LS1008 | 13:33 | 24.43 | 1350 | 155.5 | -5.7 | 29 | 1.8 | 16.2 | -22.7 | 8.4 |
| LS1009 | 13:39 | 24.00 | 1187 | 157 | -5.6 | 31 | 1.8 | 17.2 | -23.0 | 7.9 |
| LS1010 | 13:46 | 15.74 | 1038 | 160 | -5.6 | 25 | 1.8 | 13.7 | -24.3 | 7.9 |
| LS1011 | 13:55 | 21.47 | 886 | 167.5 | -5.7 | 27 | 1.9 | 14.3 | -23.4 | 7.3 |
| LS1012 | 14:06 | 18.01 | 735 | 174 | -5.6 | 29 | 1.9 | 15.0 | -24.5 | 7.4 |
| LS1013 | 14:20 | 15.35 | 597 | 184 | -5.8 | 24 | 2.0 | 12.4 | -24.5 | 7.1 |
| LS1014 | 14:38 | 12.80 | 485 | 198 | -5.7 | - | - | - | - | - |
| LS1015 | 15:14 | 10.17 | 308 | 222 | -5.9 | - | - | - | - | - |
| LS1014-15 ^b | - | - | - | - | - | 30 | 1.9 | 15.5 | -23.6 | 7.1 |

^a Time of collection, total suspended sediment load (TSS), stream discharge (Q), water electric conductivity (EC) and $\delta^{18}\text{O}$, total organic carbon in TSS (TOC), total nitrogen in TSS (TN), $\delta^{13}\text{C}$ and $\delta^{15}\text{N}$ for TSS,

^b composite sample,
- no value.

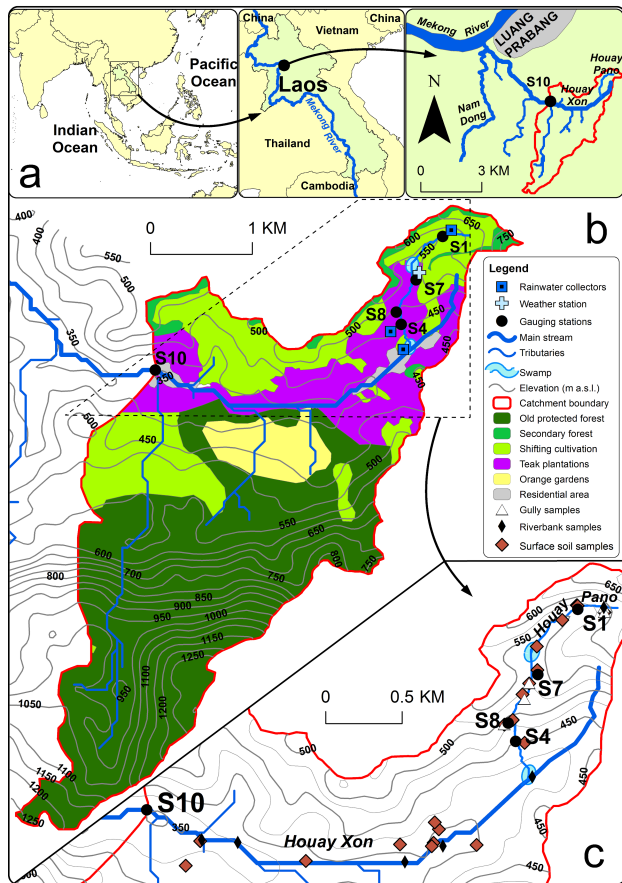


Figure 1. Location of the Houay Xon River catchment in SE Asia (a). Topographic and land use map of the Houay Xon S10 subcatchment in 2012 with location of the gauging stations (S1, S4, S7, S8, S10), rainwater collectors and automatic weather station (b), surface soil, gully and riverbank sampling locations (c).

Sources and export of particle-borne OM during a monsoon flood in a catchment of northern Laos

E. Gourdin et al.

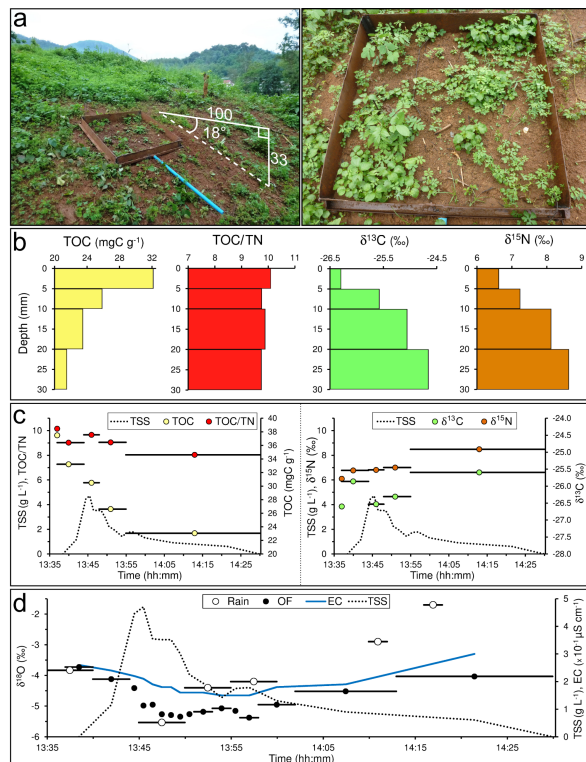


Figure 2. Microplot experiment: **(a)** presentation of the 1 m² collecting system and its vegetation cover; **(b)** distribution of topsoil total organic carbon (TOC) concentration, total organic carbon: total nitrogen ratio (TOC/TN), $\delta^{13}\text{C}$ and $\delta^{15}\text{N}$ with soil depth; **(c)** temporal evolution of the total suspended sediment load (TSS) plotted with TOC and TOC/TN in TSS (left) and with $\delta^{13}\text{C}$ and $\delta^{15}\text{N}$ in TSS (right) during the 1 June storm and **(d)** temporal evolution of the overland flow TSS load with rainwater- $\delta^{18}\text{O}$ (rain), overland flow- $\delta^{18}\text{O}$ (OF) and overland flow electric conductivity (EC) during the 1 June storm.

Sources and export of particle-borne OM during a monsoon flood in a catchment of northern Laos

E. Gourdin et al.

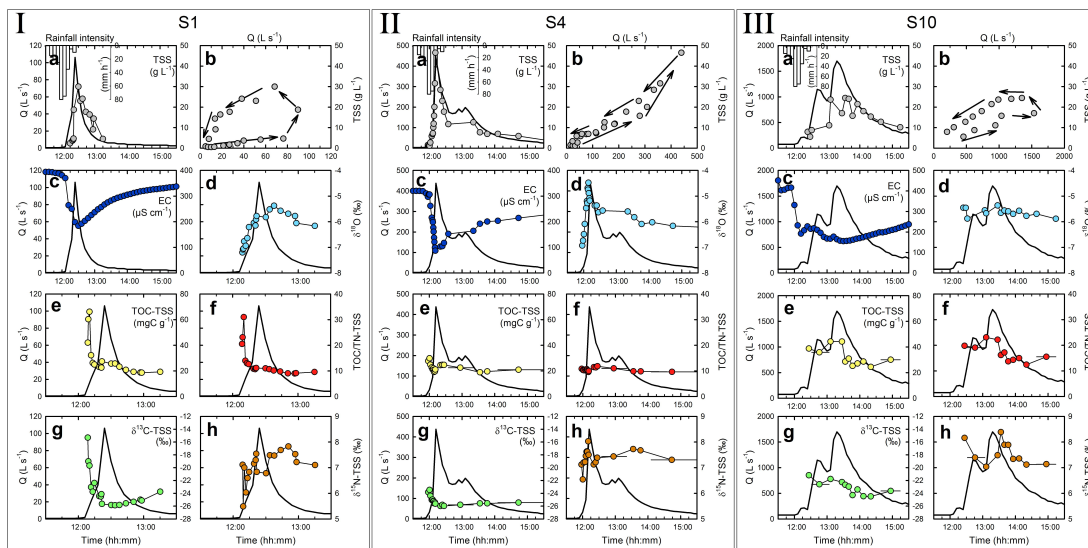


Figure 3. Plots of the temporal evolution of (a) rainfall intensity, stream discharge (Q , thicker solid line), (b) total suspended sediment load (TSS), (c) water electric conductivity (EC), (d) streamwater- $\delta^{18}\text{O}$, (e) total organic carbon concentration in the TSS (TOC-TSS), (f) total organic carbon: total nitrogen ratio in the TSS (TOC/TN-TSS), (g) $\delta^{13}\text{C}$ -TSS, (h) $\delta^{15}\text{N}$ -TSS for (I) the upstream station S1, (II) the intermediate station S4, and (III) the downstream station S10, during the 23 May flood. Horizontal bars represent sampling period for composite samples.

Title Page

Abstract

Introduction

Conclusions

References

Tables

Figures

◀

▶

◀

▶

Back

Close

Full Screen / Esc

Printer-friendly Version

Interactive Discussion

Sources and export of particle-borne OM during a monsoon flood in a catchment of northern Laos

E. Gourdin et al.

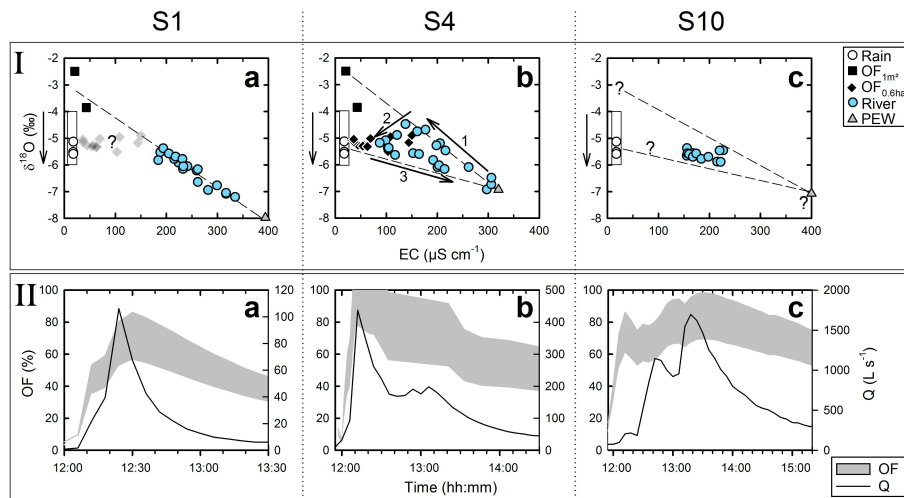


Figure 4. Plots of: (I) relationships between water electric conductivity (EC) and water $\delta^{18}\text{O}$, and (II) temporal evolution of stream water discharge (Q) with overland flow contribution estimates (OF) for (a) the upstream station S1, (b) the intermediate station S4, and (c) the downstream station S10, during the 23 May flood. In (I), open circles correspond to rainwater, filled squares to cumulative overland flow obtained with 1 m^2 plots (OF_{1m^2}), filled diamonds to overland flow from S7 and S8 hillslopes ($\text{OF}_{0.6\text{ha}}$), filled colored circles to stream water, triangles to pre-event water (PEW). The rectangle areas and vertical arrows represent the potential temporal variability of rainwater- $\delta^{18}\text{O}$ during the storm. In (II), the shaded area corresponds to the variability range for the estimated overland flow contribution.

Title Page

Abstract

Introduction

Conclusions

References

Tables

Figures

◀

▶

◀

▶

Back

Close

Full Screen / Esc

Printer-friendly Version

Interactive Discussion

Sources and export of particle-borne OM during a monsoon flood in a catchment of northern Laos

E. Gourdin et al.

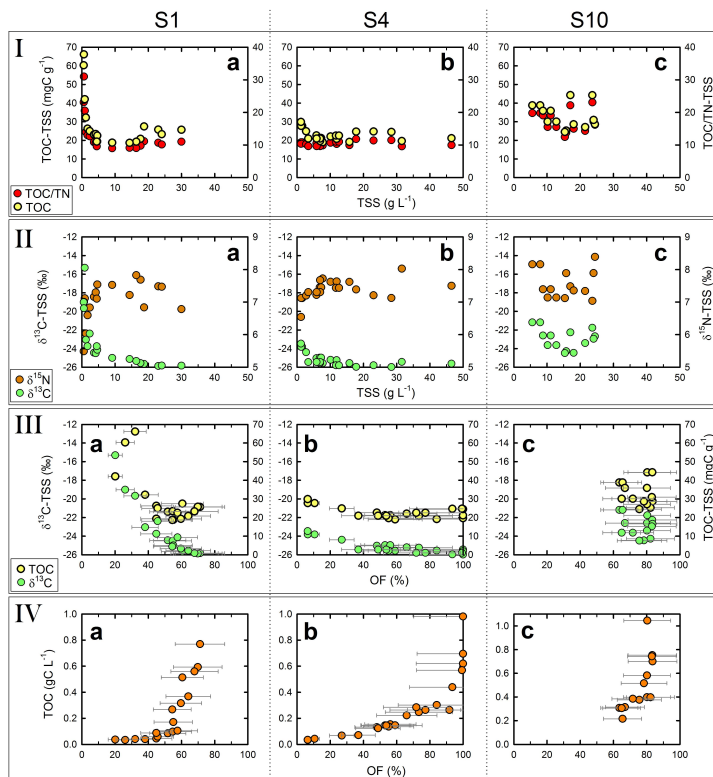


Figure 5. Relationships between total suspended sediment load (TSS), total organic carbon concentration in the TSS (TOC-TSS), total organic carbon: total nitrogen ratio in the TSS (TOC/TN-TSS), $\delta^{13}\text{C}$ -TSS, $\delta^{15}\text{N}$ -TSS, total organic carbon load (TOC) and overland flow contribution estimates (OF): **(a)** at upstream station S1 (Houay Pano Stream), **(b)** at intermediate station S4, and **(c)** at downstream station S10, during the 23 May flood. In **(III)** and **(IV)**, circles represent the median values of the variability range (horizontal bars) of estimated OF contribution.

[Title Page](#)
[Abstract](#)
[Introduction](#)
[Conclusions](#)
[References](#)
[Tables](#)
[Figures](#)
[Back](#)
[Close](#)
[Full Screen / Esc](#)
[Printer-friendly Version](#)
[Interactive Discussion](#)